

# Migration Reactivities of $\sigma$ -Bonded Ligands of Organoiron and Organcobalt Porphyrins Depending on Different High Oxidation States

Shunichi Fukuzumi,<sup>\*,†</sup> Ikuo Nakanishi,<sup>†</sup> Keiko Tanaka,<sup>†</sup> Alain Tabard,<sup>‡</sup> Roger Guillard,<sup>\*,‡</sup> Eric Van Caemelbecke,<sup>§</sup> and Karl M. Kadish<sup>\*,§</sup>

Department of Material and Life Science, Graduate School of Engineering, Osaka University, Suita, Osaka 565-0871, Japan, LIMSAG, UMR 5633, Faculté des Sciences "Gabriel", Université de Bourgogne, 6 Boulevard Gabriel, 21000 Dijon, France, and Department of Chemistry, University of Houston, Houston, Texas 77204-5641

Received March 23, 1999

Migration reactivities of  $\sigma$ -bonded organo-iron and -cobalt porphyrins were examined as a function of the compound oxidation state. Migration rates were determined for both the one-electron and two-electron oxidized species produced in the electron-transfer oxidation with different oxidants in acetonitrile at 298 K. The investigated compounds are represented as [(OETPP)Fe(R)]<sup>n+</sup>, where  $n = 1$  or 2, OETPP = the dianion of 2,3,7,8,12,13,17,18-octaethyl-5,10,15,20-tetraphenylporphyrin, and R = C<sub>6</sub>H<sub>5</sub>, 3,5-C<sub>6</sub>F<sub>2</sub>H<sub>3</sub>, or C<sub>6</sub>F<sub>5</sub>, and as [(TPP)Co(R)]<sup>n+</sup>, where  $n = 1$  or 2, TPP = the dianion of 5,10,15,20-tetraphenylporphyrin, and R = CH<sub>3</sub> or C<sub>6</sub>H<sub>5</sub>. The rapid two-electron oxidation of (OETPP)Fe<sup>III</sup>(R) occurs with [Ru(bpy)<sub>3</sub>]<sup>3+</sup> (bpy = 2,2'-bipyridine) to produce [(OETPP)Fe<sup>IV</sup>(R)]<sup>2+</sup>. The formation of this species is followed by a slow migration of the  $\sigma$ -bonded R group to a nitrogen of the porphyrin ring to give [(N-ROETPP)Fe<sup>II</sup>]<sup>2+</sup> and then by a rapid electron-transfer oxidation of the migrated product with [Ru(bpy)<sub>3</sub>]<sup>3+</sup> to yield [(N-ROETPP)Fe<sup>III</sup>]<sup>3+</sup> as a final product. When [Ru(bpy)<sub>3</sub>]<sup>3+</sup> is replaced by a much weaker oxidant such as ferricenium ion, only the one-electron oxidation of (OETPP)Fe(R) occurs to produce [(OETPP)Fe<sup>IV</sup>(R)]<sup>+</sup>. A migration of the R group also occurs in the one-electron oxidized porphyrin species, [(OETPP)Fe<sup>IV</sup>(R)]<sup>+</sup>, to produce [(N-ROETPP)Fe<sup>II</sup>]<sup>+</sup>, which is rapidly oxidized by ferricenium ion to yield [(N-ROETPP)Fe<sup>III</sup>]<sup>2+</sup>. The migration rate of the R group in [(OETPP)Fe<sup>IV</sup>(R)]<sup>+</sup> is about 10<sup>4</sup> times slower than the migration rate of the corresponding two-electron oxidized species, [(OETPP)Fe<sup>IV</sup>(R)]<sup>2+</sup>. The migration rate of the  $\sigma$ -bonded ligand of [(TPP)Co<sup>IV</sup>(R)]<sup>+</sup>, produced by the one-electron oxidation of (TPP)Co<sup>III</sup>(R) with [Fe(phen)<sub>3</sub>]<sup>3+</sup> (phen = 1,10-phenanthroline) is also about 10<sup>4</sup> times slower than the migration rate of the R group in the corresponding two-electron oxidized species, [(TPP)Co<sup>IV</sup>(R)]<sup>2+</sup>, which is produced by the two-electron oxidation with [Ru(bpy)<sub>3</sub>]<sup>3+</sup>. A comparison of the migration rates with the oxidation states of the porphyrins indicates that the migration occurs via an intramolecular electron transfer from the R group to the Fe(IV) or Co(IV) metal of the organometallic porphyrin.

The cleavage of metal–carbon bonds in organometallic compounds plays an essential role in a number of oxidative catalytic reactions, including biological processes.<sup>1–9</sup> In par-

ticular, cleavage of iron–carbon bonds in organoiron porphyrins has been recognized as a key step in several biological processes such as heme inactivation in hemoglobin, myoglobin, cytochrome P-450 and catalase.<sup>3,4,8–10</sup> A number of organoiron(III) porphyrins possessing  $\sigma$ -bonded alkyl or aryl axial ligands have so far been synthesized to disclose the thermal stability of the iron(III)–carbon bonds.<sup>3,9,11–16</sup> When the porphyrins are subjected to oxidation, however, the otherwise stable iron–carbon bond may be cleaved as part of a migration of the  $\sigma$ -bonded ligand from the iron to one of the four porphyrin ring nitrogens,

<sup>†</sup> Osaka University.

<sup>‡</sup> Université de Bourgogne.

<sup>§</sup> University of Houston.

- (1) (a) Kochi, J. K. *Organometallic Mechanisms and Catalysis*; Academic Press: New York, 1978. (b) Masters, C. *Homogeneous Transition-metal Catalysis*; Chapman and Hall: London, 1981. (c) Parshall, G. W. *Homogeneous Catalysis. The Applications and Chemistry of Catalysis by Soluble Transition Metal Complexes*; Wiley: New York, 1980.
- (2) (a) Schneider, Z.; Stroinski, A. *Comprehensive B12*; de Gruyter: Berlin, 1987. (b) Halpern, J. *Science* **1985**, 227, 869. (c) Toscano, P. J.; Marzilli, L. G. *Prog. Inorg. Chem.* **1984**, 31, 105. (d) Patternden, G. *Chem. Soc. Rev.* **1988**, 17, 361.
- (3) (a) Dolphin, D.; Traylor, T. G.; Xie, L. Y. *Acc. Chem. Res.* **1997**, 30, 251. (b) Traylor, T. G. *Pure Appl. Chem.* **1991**, 63, 265. (c) *Cytochrome P-450: Structure, Mechanism and Biochemistry*, 2nd ed.; Ortiz de Montellano, P. R., Ed.; Plenum Press: New York, 1995. (d) Ortiz de Montellano, P. R. *Acc. Chem. Res.* **1987**, 20, 289.
- (4) (a) Mansuy, D.; Battioni, P. In *Metalloporphyrins in Catalytic Oxidations*; Sheldon, R. A., Ed.; Marcel Dekker: New York, 1994; pp 99–132. (b) Mansuy, D. *Pure Appl. Chem.* **1987**, 59, 759. (c) Mansuy, D. *Coord. Chem. Rev.* **1993**, 125, 129.
- (5) (a) Meunier, B. *Chem. Rev.* **1992**, 92, 1411. (b) Pitié, M.; Bernadou, J.; Meunier, B. *J. Am. Chem. Soc.* **1995**, 117, 2935.

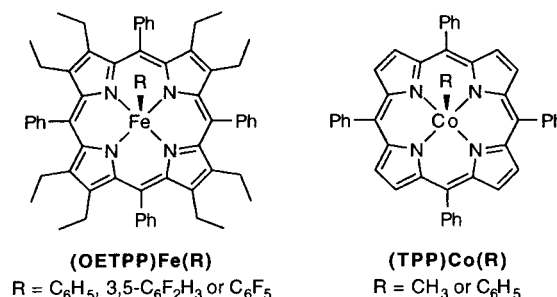
- (6) (a) Bruce, T. C. *Acc. Chem. Res.* **1991**, 24, 243. (b) Ostovic, D.; Bruce, T. C. *Acc. Chem. Res.* **1992**, 25, 314. (c) Dunford, H. B. *Adv. Inorg. Biochem.* **1982**, 4, 41.
- (7) (a) Guengerich, F. P.; Macdonald, T. L. *Acc. Chem. Res.* **1984**, 17, 9. (b) Guengerich, F. P.; Macdonald, T. L. In *Advances in Electron-Transfer Chemistry*; Mariano, P. S., Ed.; JAI Press: Greenwich, CT, 1993; Vol. 3, pp 191–241. (c) Guengerich, F. P.; Yun, C.-H.; Macdonald, T. L. *J. Biol. Chem.* **1996**, 271, 27321.
- (8) Brothers, P. J.; Collman, J. P. *Acc. Chem. Res.* **1986**, 19, 209.
- (9) Lavalee, D. K. *The Chemistry and Biochemistry of N-Substituted Porphyrins*; VCH Publishers: New York, 1987.
- (10) Saito, S.; Itano, H. A. *Proc. Natl. Acad. Sci. U.S.A.* **1981**, 78, 5508.
- (11) Guillard, R.; Lecomte, C.; Kadish, K. M. *Struct. Bonding* **1987**, 64, 205.
- (12) Guillard, R.; Kadish, K. M. *Chem. Rev.* **1988**, 88, 1121.

leading to the formation of *N*-substituted porphyrins.<sup>3,4,8,9,12,17</sup> The cobalt–carbon bond of  $\sigma$ -bonded organocobalt(III) porphyrins is also known to be cleaved upon chemical and electrochemical oxidation and this brings about a metal to nitrogen migration of the  $\sigma$ -bonded organic ligand.<sup>18–21</sup>

Although a number of factors will affect the stability of the metal–carbon bond in oxidized  $\sigma$ -bonded organometallic porphyrins (such as the type of  $\sigma$ -bonded organic ligand, the type of porphyrin macrocycle, and the presence of a sixth axial base ligand), the occurrence or absence of migration following the metal–carbon bond cleavage will also depend on the metal porphyrin oxidation state.<sup>18–25</sup> For example, a migration of the  $\sigma$ -bonded axial ligand has been reported to occur after the first one-electron oxidation of (P)Fe<sup>III</sup>(C<sub>6</sub>H<sub>5</sub>), where P = the dianion of 2,3,7,8,12,13,17,18-octaethylporphyrin (OEP) or 5,10,15,20-tetraphenylporphyrin (TPP).<sup>22–25</sup> In the case of (OETPP)-Fe(C<sub>6</sub>H<sub>5</sub>) (where OETPP = the dianion of 2,3,7,8,12,13,17,18-octaethyl-5,10,15,20-tetraphenylporphyrin), however, the migration is observed only after the second one-electron oxidation, and the electrochemical one-electron oxidation of (OETPP)Fe<sup>III</sup>-(C<sub>6</sub>H<sub>5</sub>) yields [(OETPP)Fe<sup>IV</sup>(C<sub>6</sub>H<sub>5</sub>)]<sup>+</sup>, which is stable on the cyclic voltammetry or controlled-potential electrolysis time scale.<sup>25,26</sup> The electrochemical generation of oxidized  $\sigma$ -bonded organometallic porphyrins has been coupled with a quantitative determination of the migration reactivities of the  $\sigma$ -bonded ligands but no kinetic comparison between the reactivities of singly and doubly oxidized organometallic porphyrins with different central metals, different  $\sigma$ -bonded axial ligands, and different porphyrin macrocycles has yet been reported.

In this study, we have focused our attention on how changes in the oxidation state of the singly and doubly oxidized porphyrin complex are reflected in migration rate constants of  $\sigma$ -bonded R ligands of [(OETPP)Fe(R)]<sup>n+</sup> (R = C<sub>6</sub>H<sub>5</sub>, 3,5-C<sub>6</sub>F<sub>2</sub>H<sub>3</sub>, or C<sub>6</sub>F<sub>5</sub>) and [(TPP)Co(R)]<sup>n+</sup> (R = CH<sub>3</sub> or C<sub>6</sub>H<sub>5</sub>) where *n* = 1 or 2 (Chart 1).

Chart 1



The choice of an appropriate chemical oxidant that can oxidize the organometallic porphyrins to produce the one-electron or two-electron oxidized species<sup>27</sup> enables us to selectively determine rate constants for the migration reactions of both the singly and doubly oxidized porphyrin complexes for the first time by monitoring directly the spectroscopic changes as the reaction proceeds. The migration rate constants span a range of 10<sup>7</sup> and vary with the oxidation state of the porphyrin complex, the nature of the  $\sigma$ -bonded axial ligand, and the nature of the porphyrin macrocycle. The large range of magnitude in the migration rate constants provides valuable insights into factors that control the stability of the metal–carbon bond and helps to elucidate the steps involved in the migration mechanism.

## Experimental Section

**Materials.** Free base (OETPP)H<sub>2</sub> was prepared from benzaldehyde and 3,4-diethylpyrrole in the presence of BF<sub>3</sub>·OEt<sub>2</sub>, followed by oxidation of a resulting porphyrinogen with 2,3-dichloro-5,6-dicyano-1,4-benzoquinone as described in the literature.<sup>28</sup> Iron was inserted by use of ferrous chloride tetrahydrate in deoxygenated dimethylformamide and the formation of (OETPP)FeCl was confirmed by <sup>1</sup>H NMR as described elsewhere.<sup>29</sup> The (OETPP)Fe(R) complexes (R = C<sub>6</sub>H<sub>5</sub>, 3,5-C<sub>6</sub>F<sub>2</sub>H<sub>3</sub>, or C<sub>6</sub>F<sub>5</sub>) were prepared by reacting the corresponding aryl Grignard reagent with (OETPP)FeCl according to literature procedures.<sup>25,26,30</sup> Cobalt(II) tetraphenylporphyrin, (TPP)Co, was prepared as described in the literature<sup>31</sup> and then oxidized by oxygen in methanol containing HCl to obtain the tetraphenylporphyrinocobalt(III) chloride complex, (TPP)CoCl, which was further purified by recrystallization from methanol. Methylcobalt(III) tetraphenylporphyrin, (TPP)Co(CH<sub>3</sub>), was prepared from a reaction between methylhydrazine and (TPP)-CoCl followed by oxidation of the resulting intermediate by oxygen.<sup>23</sup> (TPP)Co(C<sub>6</sub>H<sub>5</sub>) was prepared according to literature procedures.<sup>32</sup> Tris-(2,2'-bipyridine)ruthenium dichloride hexahydrate, [Ru(bpy)<sub>3</sub>]Cl<sub>2</sub>·6H<sub>2</sub>O, was obtained commercially from Aldrich. The oxidation of [Ru(bpy)<sub>3</sub>]Cl<sub>2</sub> with lead dioxide in aqueous H<sub>2</sub>SO<sub>4</sub> gives [Ru(bpy)<sub>3</sub>]<sup>3+</sup>, which was isolated as the PF<sub>6</sub><sup>-</sup> salt, [Ru(bpy)<sub>3</sub>](PF<sub>6</sub>)<sub>3</sub>.<sup>27,33</sup> The tris(1,10-phenanthroline)iron(II) complex was prepared by adding 3 equiv of 1,10-phenanthroline (monohydrated) to an aqueous solution of ferrous sulfate.<sup>34</sup> Tris(1,10-phenanthroline)iron(III) perchlorate, [Fe(phen)<sub>3</sub>]-

- (13) (a) Arasasingham, R. D.; Balch, A. L.; Latos-Grazynski, L. *J. Am. Chem. Soc.* **1987**, *109*, 5846. (b) Arasasingham, R. D.; Balch, A. L.; Cornman, C. R.; Latos-Grazynski, L. *J. Am. Chem. Soc.* **1989**, *111*, 4357. (c) Balch, A. L.; Hart, R. L.; Latos-Grazynski, L.; Traylor, T. G. *J. Am. Chem. Soc.* **1990**, *112*, 7382. (d) Arasasingham, R. D.; Balch, A. L.; Hart, R. L.; Latos-Grazynski, L. *J. Am. Chem. Soc.* **1990**, *112*, 7566.
- (14) Setsune, J.-i.; Ishimaru, Y.; Sera, A. *J. Chem. Soc., Chem. Commun.* **1992**, 328.
- (15) (a) Arafa, I. M.; Shin, K.; Goff, H. M. *J. Am. Chem. Soc.* **1988**, *110*, 5228. (b) Shin, K.; Yu, B.-S.; Goff, H. M. *Inorg. Chem.* **1990**, *29*, 889. (c) Li, Z.; Goff, H. M. *Inorg. Chem.* **1992**, *31*, 1547.
- (16) (a) Lexa, D.; Misselt, J.; Savéant, J.-M. *J. Am. Chem. Soc.* **1981**, *103*, 6806. (b) Gueutin, C.; Lexa, D.; Momenteau, M.; Savéant, J.-M. *J. Am. Chem. Soc.* **1990**, *112*, 1874.
- (17) (a) Collman, J. P.; Hampton, P. D.; Brauman, J. I. *J. Am. Chem. Soc.* **1990**, *112*, 2977. (b) Collman, J. P.; Hampton, P. D.; Brauman, J. I. *J. Am. Chem. Soc.* **1990**, *112*, 2986.
- (18) Dolphin, D.; Halko, D. J.; Johnson, E. *Inorg. Chem.* **1981**, *20*, 4348.
- (19) (a) Callot, H. J.; Cromer, R.; Louati, R. A.; Gross, M. *Nouv. J. Chem.* **1984**, *8*, 765. (b) Callot, H. J.; Metz, F. *J. Chem. Soc., Chem. Commun.* **1982**, 947. (c) Callot, H. J.; Cromer, R. *Tetrahedron Lett.* **1985**, *26*, 3357.
- (20) Kadish, K. M.; Han, B. C.; Endo, A. *Inorg. Chem.* **1991**, *30*, 4502.
- (21) Fukuzumi, S.; Miyamoto, K.; Suenobu, T.; Van Caemelbecke, E.; Kadish, K. M. *J. Am. Chem. Soc.* **1998**, *120*, 2880.
- (22) Lançon, D.; Cocolios, P.; Guillard, R.; Kadish, K. M. *J. Am. Chem. Soc.* **1984**, *106*, 4472.
- (23) Mansuy, D.; Battioni, J.-P.; Dupré, D.; Sartori, E. *J. Am. Chem. Soc.* **1982**, *104*, 6159.
- (24) Kadish, K. M.; Van Caemelbecke, E.; Gueletii, E.; Fukuzumi, S.; Miyamoto, K.; Suenobu, T.; Tabard, A.; Guillard, R. *Inorg. Chem.* **1998**, *37*, 1759.
- (25) Kadish, K. M.; Van Caemelbecke, E.; D'Souza, F.; Medforth, C. J.; Smith, K. M.; Tabard, A.; Guillard, R. *Organometallics* **1993**, *12*, 2411.
- (26) Kadish, K. M.; Van Caemelbecke, E.; D'Souza, F.; Medforth, C. J.; Smith, K. M.; Tabard, A.; Guillard, R. *Inorg. Chem.* **1995**, *34*, 2984.

- (27) Fukuzumi, S.; Nakanishi, I.; Tanaka, K.; Suenobu, T.; Tabard, A.; Guillard, R.; Van Caemelbecke, E.; Kadish, K. M. *J. Am. Chem. Soc.* **1999**, *121*, 785.
- (28) (a) Barkigia, K. M.; Berber, M. D.; Fajer, J.; Medforth, C. J.; Renner, M. W.; Smith, K. M. *J. Am. Chem. Soc.* **1990**, *112*, 8851. (b) Medforth, C. J.; Smith, K. M. *Tetrahedron Lett.* **1990**, *31*, 5583. (c) Lindsey, J. S.; Schreiman, I. C.; Hsu, H. C.; Kearney, P. C.; Marguerettaz, A. M. *J. Org. Chem.* **1987**, *52*, 827.
- (29) Sparks, L. D.; Medforth, C. J.; Park, M.-S.; Chamberlain, J. R.; Ondrias, M. R.; Senge, M. O.; Smith, K. M.; Shelnutt, J. A. *J. Am. Chem. Soc.* **1993**, *115*, 581.
- (30) Guillard, R.; Boisselier-Cocolios, B.; Tabard, A.; Cocolios, P.; Simonet, B.; Kadish, K. M. *Inorg. Chem.* **1985**, *24*, 2509.
- (31) Shirazi, A.; Goff, H. M. *Inorg. Chem.* **1982**, *21*, 3420.
- (32) Callot, H. J.; Metz, F.; Cromer, R. *Nouv. J. Chem.* **1984**, *8*, 759.
- (33) DeSimone, R. E.; Drago, R. S. *J. Am. Chem. Soc.* **1970**, *92*, 2343.
- (34) Wong, C. L.; Kochi, J. K. *J. Am. Chem. Soc.* **1979**, *101*, 5593.

(ClO<sub>4</sub>)<sub>3</sub>, was prepared by oxidizing the corresponding iron(II) complex with ceric ammonium sulfate or lead dioxide in aqueous H<sub>2</sub>SO<sub>4</sub> followed by the addition of NaClO<sub>4</sub>.<sup>34</sup> Ferrocene derivatives (ferrocene, 1,1'-dimethylferrocene, *n*-butylferrocene, and acetylferrocene) were obtained commercially and purified by sublimation or recrystallization from ethanol. Ferricenium ion was prepared by the oxidation of ferrocene by *p*-benzoquinone in the presence of HClO<sub>4</sub> in MeCN.<sup>35</sup> Tetra-*n*-butylammonium perchlorate (TBAP) was purchased from Sigma Chemical Co., recrystallized from ethyl alcohol, and dried under vacuum at 40 °C prior to use. Acetonitrile (MeCN) was purchased from Wako Pure Chemical Ind. Ltd., and purified by successive distillation over CaH<sub>2</sub> and P<sub>2</sub>O<sub>5</sub> according to standard procedures.<sup>36</sup>

**Caution!** Although we have experienced no difficulties with the perchlorate salts, they should be regarded as potentially explosive and handled with care.

**Spectral and Kinetic Measurements.** Typically, a 10  $\mu$ L aliquot of [Ru(bpy)<sub>3</sub>](PF<sub>6</sub>)<sub>3</sub> ( $3.0 \times 10^{-3}$  M) in MeCN was added to a quartz cuvette (10 mm i.d.) that contained (OETPP)Fe(C<sub>6</sub>H<sub>5</sub>) ( $5.0 \times 10^{-6}$  M) in deaerated MeCN (3.0 mL). This led to the oxidation of (OETPP)Fe(C<sub>6</sub>H<sub>5</sub>) with [Ru(bpy)<sub>3</sub>]<sup>3+</sup> accompanied by a migration of the phenyl group to a nitrogen of the porphyrin ring. The UV–visible spectral changes for the reaction of (OETPP)Fe(C<sub>6</sub>H<sub>5</sub>) with different concentrations of [Ru(bpy)<sub>3</sub>]<sup>3+</sup> were monitored with a Shimadzu UV-2200 spectrophotometer, a Hewlett-Packard 8452A diode-array spectrophotometer or a Hewlett-Packard 8453 diode array spectrophotometer. The stoichiometry for the oxidation of (OETPP)Fe(C<sub>6</sub>H<sub>5</sub>) with [Ru(bpy)<sub>3</sub>]<sup>3+</sup> was determined from the spectral titration during formation of [Ru(bpy)<sub>3</sub>]<sup>2+</sup> ( $\lambda_{\text{max}} = 287$  nm,  $\epsilon = 7.90 \times 10^4$  M<sup>-1</sup> cm<sup>-1</sup>).<sup>33</sup> The same procedure was employed for spectral measurements during oxidation of other  $\sigma$ -bonded iron porphyrins. All measurements were carried out in a dark cell compartment under deaerated conditions.

Kinetic measurements of the electron transfer from (OETPP)Fe(R) and (TPP)Co(R) to [Ru(bpy)<sub>3</sub>](PF<sub>6</sub>)<sub>3</sub> and the following migration of the  $\sigma$ -bonded R group to a nitrogen of the porphyrin ring were performed with a Union RA-103 stopped-flow spectrophotometer under deaerated conditions. Typically, deaerated MeCN solutions of (OETPP)Fe(C<sub>6</sub>H<sub>5</sub>) and [Ru(bpy)<sub>3</sub>](PF<sub>6</sub>)<sub>3</sub> were transferred to the spectrophotometric cell by means of a glass syringe that had earlier been purged with a stream of argon. The rates of migration of the  $\sigma$ -bonded R group to a nitrogen of the porphyrin ring following the rapid two-electron oxidation of (OETPP)Fe(C<sub>6</sub>H<sub>5</sub>) with [Ru(bpy)<sub>3</sub>]<sup>3+</sup> in deaerated MeCN at 298 K were determined by monitoring an increase in absorbance at 287 nm ( $\epsilon = 7.90 \times 10^4$  M<sup>-1</sup> cm<sup>-1</sup>)<sup>27,33</sup> due to [Ru(bpy)<sub>3</sub>]<sup>2+</sup> formation. The migration rates of [(TPP)Co(R)]<sup>2+</sup> produced by the two-electron oxidation of (TPP)Co(R) with excess [Ru(bpy)<sub>3</sub>]<sup>3+</sup> were determined by monitoring the increase in absorbance of the resulting migrated complex, [(*N*-RTPP)Co]<sup>2+</sup>.<sup>22</sup> Migration rate constants of the doubly oxidized organometallic porphyrins were determined from pseudo-first-order plots in the presence of a large excess of [Ru(bpy)<sub>3</sub>]<sup>3+</sup>. The first-order plots of  $\ln(A_{\infty} - A)$  vs time ( $A_{\infty}$  and  $A$  are the final absorbance and the absorbance at each reaction time, respectively) were linear for three or more half-lives with the correlation coefficient  $\rho > 0.999$ .

The slow migration rates of the singly oxidized iron complex, [(OETPP)Fe(C<sub>6</sub>H<sub>5</sub>)]<sup>+</sup>, produced by electron transfer from (OETPP)Fe(C<sub>6</sub>H<sub>5</sub>) to ferricenium ions in MeCN at 298 K were determined with use of a Shimadzu UV-2200 spectrophotometer by monitoring an increase in absorbance at 721 nm due to [(*N*-C<sub>6</sub>H<sub>5</sub>OETPP)Fe]<sup>2+</sup> formation.<sup>26</sup> Ferricenium ion derivatives were generated by oxidation of the corresponding ferrocene derivative with 1 equivalent of [Ru(bpy)<sub>3</sub>]<sup>3+</sup> in deaerated MeCN.

**Cyclic Voltammetry.** Cyclic voltammetry measurements were undertaken under deaerated conditions with a three-electrode system and a BAS 100B electrochemical analyzer.  $E_{\text{red}}^0$  values of the chemical oxidants were determined at room temperature in MeCN containing 0.1 M TBAP as supporting electrolyte. The  $E_{\text{ox}}^0$  value of (OETPP)Fe(3,5-C<sub>6</sub>F<sub>2</sub>H<sub>3</sub>) was determined by cyclic voltammetry in PhCN instead

**Table 1.** Oxidation Potentials of (OETPP)Fe(R) and (TPP)Co(R) at 298 K<sup>a</sup>

investigated porphyrin	$E_{\text{ox}(1)}^0$ , V	$E_{\text{ox}(2)}^0$ , V
(OETPP)Fe(C <sub>6</sub> H <sub>5</sub> )	0.27	1.06
(OETPP)Fe(3,5-C <sub>6</sub> F <sub>2</sub> H <sub>3</sub> )	0.39	0.93
(OETPP)Fe(C <sub>6</sub> F <sub>5</sub> )	0.56	0.80
(TPP)Co(CH <sub>3</sub> )	0.84 <sup>b,c</sup>	1.20 <sup>c</sup>
(TPP)Co(C <sub>6</sub> H <sub>5</sub> )	0.79 <sup>b,d</sup>	1.11 <sup>d</sup>
(TPP)Co(C <sub>2</sub> H <sub>5</sub> )	0.83 <sup>b,d,e</sup>	0.97 <sup>d</sup>
(TPP)Co( <i>n</i> -C <sub>4</sub> H <sub>9</sub> )	0.84 <sup>b,d,e</sup>	0.97 <sup>d</sup>

<sup>a</sup> All potentials of (OETPP)Fe(R) were measured in PhCN containing 0.10 M TBAP, while those of (TPP)Co(R) are as indicated in the table. The experimental error is within  $\pm 0.005$  V. <sup>b</sup> Taken from ref 21.

<sup>c</sup> Measured in MeCN/CHCl<sub>3</sub> (1:4 v/v) containing 0.10 M TBAP. <sup>d</sup> Measured in MeCN/CHCl<sub>3</sub> (4:1 v/v). <sup>e</sup> Anodic peak potential.

of MeCN because of a low solubility problem as previously reported for other (OETPP)Fe(R) derivatives.<sup>26,27</sup> Cyclic voltammetry was also used to determine the one-electron oxidation potential of [(*N*-C<sub>6</sub>H<sub>5</sub>OETPP)Fe]<sup>2+</sup> in MeCN after generation of the product by reaction of (OETPP)Fe(C<sub>6</sub>H<sub>5</sub>) ( $1.0 \times 10^{-3}$  M) with ferricenium ion ( $2.0 \times 10^{-3}$  M). The working electrode and counterelectrodes were platinum, while Ag/AgNO<sub>3</sub> (0.01 M) was used as the reference electrode. All potentials are reported in volts vs SCE. The  $E_{\text{red}}^0$  value of ferrocene used as a standard is 0.37 V vs SCE in PhCN or MeCN under our solution conditions.

## Results and Discussion

**Oxidation of (OETPP)Fe(R) with 2 Equiv of [Ru(bpy)<sub>3</sub>]<sup>3+</sup>.** Table 1 lists the oxidation potentials of (OETPP)Fe(R) (R = C<sub>6</sub>H<sub>5</sub>, 3,5-C<sub>6</sub>F<sub>2</sub>H<sub>3</sub>, or C<sub>6</sub>F<sub>5</sub>)<sup>26,27</sup> and (TPP)Co(R) (R = CH<sub>3</sub> or C<sub>6</sub>H<sub>5</sub>)<sup>21</sup> as determined by cyclic voltammetry (CV) in PhCN or a MeCN/CHCl<sub>3</sub> mixed solvent containing 0.10 M TBAP. The singly oxidized complex, [(OETPP)Fe(C<sub>6</sub>H<sub>5</sub>)]<sup>+</sup>, is well-characterized as an iron(IV) species by its UV–visible and <sup>1</sup>H NMR spectra.<sup>25–27</sup> The [(OETPP)Fe(C<sub>6</sub>H<sub>5</sub>)]<sup>+</sup> derivative has absorption bands at 357, 426, and 538 nm and lacks bands between 600 and 800 nm that would be diagnostic of a porphyrin  $\pi$  radical cation. The <sup>1</sup>H NMR and ESR spectra of [(OETPP)Fe(C<sub>6</sub>H<sub>5</sub>)]<sup>+</sup> also indicate the compound to be an *S* = 1 phenyliron(IV) complex.<sup>25</sup> The further oxidation of [(OETPP)Fe<sup>IV</sup>(C<sub>6</sub>H<sub>5</sub>)]<sup>+</sup> leads to an Fe(IV) porphyrin  $\pi$  radical cation, [(OETPP)Fe<sup>IV</sup>(C<sub>6</sub>H<sub>5</sub>)]<sup>2+</sup>, in which the porphyrin ring is oxidized.<sup>25–27</sup>

The one-electron reduction potential of [Ru(bpy)<sub>3</sub>]<sup>3+</sup> ( $E_{\text{red}}^0 = 1.24$  V)<sup>27</sup> in MeCN is significantly more positive than the second one-electron oxidation potential of (OETPP)Fe(C<sub>6</sub>H<sub>5</sub>) ( $E_{\text{ox}(2)}^0 = 1.06$  V). Thus, the two-electron oxidation of (OETPP)Fe(C<sub>6</sub>H<sub>5</sub>) with [Ru(bpy)<sub>3</sub>]<sup>3+</sup> is energetically feasible to produce [(OETPP)Fe(C<sub>6</sub>H<sub>5</sub>)]<sup>2+</sup>. The first metal-centered oxidation is the rate-determining step for the two-electron oxidation, since the reorganization energy for the metal-centered oxidation is significantly larger than the energy for the ligand-centered oxidation.<sup>27</sup>

Upon mixing 2 equiv of [Ru(bpy)<sub>3</sub>]<sup>3+</sup> with an MeCN solution of (OETPP)Fe(C<sub>6</sub>H<sub>5</sub>), the Soret band of (OETPP)Fe(C<sub>6</sub>H<sub>5</sub>) at 431 nm disappears as new absorption bands at 426, 486, and 721 nm appear as shown in Figure 1. This rapid reaction is then followed by a much slower process in which the absorption band at 426 nm decays, accompanied by an increase in the absorption bands at 486 and 721 nm. The absorption band at 426 nm has been assigned to the singly oxidized complex, [(OETPP)Fe(C<sub>6</sub>H<sub>5</sub>)]<sup>+</sup>.<sup>26,27</sup> The absorption bands at 486 and 721 nm are diagnostic of [(*N*-C<sub>6</sub>H<sub>5</sub>OETPP)Fe]<sup>2+</sup>, which is produced after a migration of the phenyl group from iron(IV) to one of the four nitrogens of the porphyrin ring

(35) Ishikawa, K.; Fukuzumi, S.; Goto, T.; Tanaka, T. *J. Am. Chem. Soc.* **1990**, *112*, 1577.

(36) Perrin, D. D.; Armarego, W. L. F.; Perrin, D. R. *Purification of Laboratory Chemicals*; Pergamon Press: Elmsford, 1966.

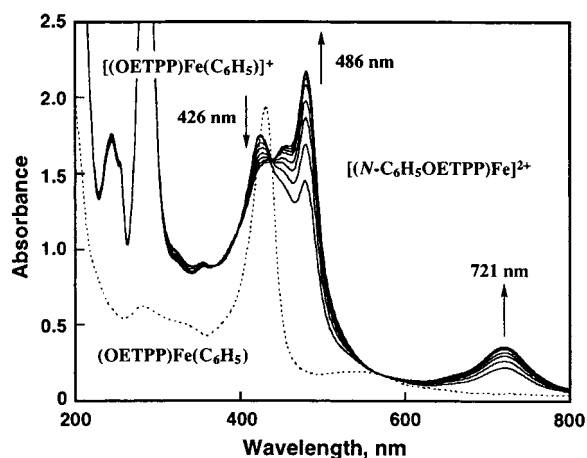
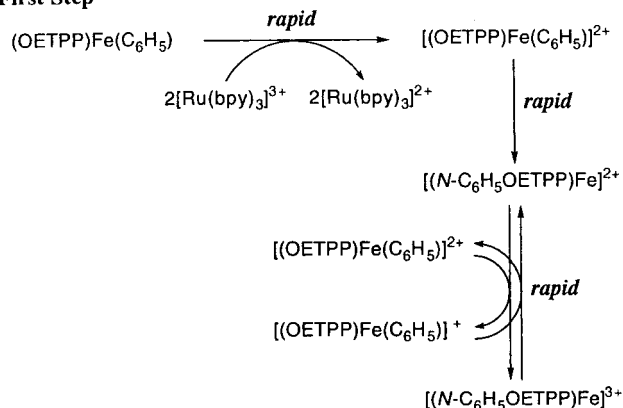


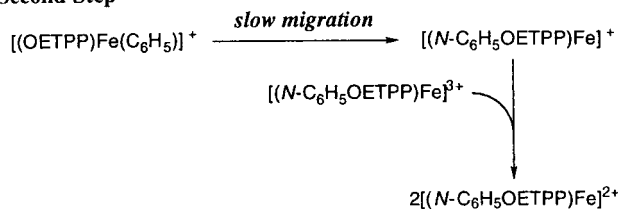
**Figure 1.** Spectral changes after electron transfer from (OETPP)Fe-(C<sub>6</sub>H<sub>5</sub>) (dashed line,  $1.9 \times 10^{-5}$  M) to [Ru(bpy)<sub>3</sub>]<sup>3+</sup> ( $3.8 \times 10^{-5}$  M) in deaerated MeCN at 298 K. Interval: 2500 s.

### Scheme 1

### First Step

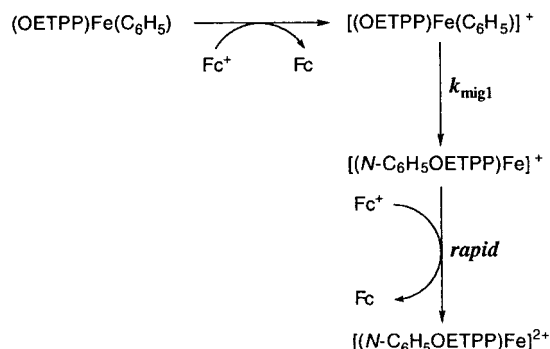


## Second Step



of the doubly oxidized complex, [(OETPP)Fe(C<sub>6</sub>H<sub>5</sub>)]<sup>2+</sup>.<sup>25–27</sup> The two-step reaction observed in the oxidation of (OETPP)Fe(C<sub>6</sub>H<sub>5</sub>) with 2 equiv of [Ru(bpy)<sub>3</sub>]<sup>3+</sup> (Figure 1) can be explained by Scheme 1. In the first step, the rapid two-electron oxidation of (OETPP)Fe(C<sub>6</sub>H<sub>5</sub>) occurs to produce [(OETPP)Fe(C<sub>6</sub>H<sub>5</sub>)]<sup>2+</sup>.<sup>27</sup> This is followed by the rapid migration of the phenyl group from iron to nitrogen to yield [(N-C<sub>6</sub>H<sub>5</sub>OETPP)Fe]<sup>2+</sup>. This is the reason why [(N-C<sub>6</sub>H<sub>5</sub>OETPP)Fe]<sup>2+</sup> (λ<sub>max</sub> = 486 and 721 nm)<sup>26</sup> is produced upon mixing of the two reactants. The instantaneous formation of [(OETPP)Fe(C<sub>6</sub>H<sub>5</sub>)]<sup>+</sup> (λ<sub>max</sub> = 426 nm)<sup>26,27</sup> despite the use of 2 equiv of [Ru(bpy)<sub>3</sub>]<sup>3+</sup> in Figure 1 indicates the occurrence of an electron transfer between [(N-C<sub>6</sub>H<sub>5</sub>OETPP)Fe]<sup>2+</sup> and [(OETPP)Fe(C<sub>6</sub>H<sub>5</sub>)]<sup>2+</sup> to yield [(N-C<sub>6</sub>H<sub>5</sub>OETPP)Fe]<sup>3+</sup> and [(OETPP)Fe(C<sub>6</sub>H<sub>5</sub>)]<sup>+</sup> (Scheme 1). The one-electron oxidation potential of [(N-C<sub>6</sub>H<sub>5</sub>OETPP)Fe]<sup>2+/3+</sup> is determined as 1.16 V (see Experimental Section), which is slightly more positive than the one-electron reduction potential of [(OETPP)Fe(C<sub>6</sub>H<sub>5</sub>)]<sup>2+</sup> (1.06 V, see Table 1). Thus, the electron transfer between [(N-C<sub>6</sub>H<sub>5</sub>OETPP)Fe]<sup>2+</sup> and [(OETPP)-

### Scheme 2



$\text{Fe}(\text{C}_6\text{H}_5)]^{2+}$  may be in equilibrium.<sup>37</sup> On the other hand, the oxidation of  $(\text{OETPP})\text{Fe}(\text{C}_6\text{H}_5)$  by more than 3 equiv of  $[\text{Ru}(\text{bpy})_3]^{3+}$  ( $E_{\text{red}}^0 = 1.24 \text{ V}$ )<sup>27</sup> results in selective formation of  $[(N\text{-C}_6\text{H}_5\text{OETPP})\text{Fe}]^{3+}$  ( $\lambda_{\text{max}} = 429 \text{ nm}$ ).

In a second step, there is a slow migration of the phenyl group to nitrogen in the singly oxidized complex  $[(\text{OETPP})\text{Fe}(\text{C}_6\text{H}_5)]$  to produce  $[(\text{N-C}_6\text{H}_5\text{OETPP})\text{Fe}]^+$ , which is rapidly oxidized by  $[(\text{N-C}_6\text{H}_5\text{OETPP})\text{Fe}]^{3+}$  to yield 2 equiv of  $[(\text{N-C}_6\text{H}_5\text{OETPP})\text{Fe}]^{2+}$  (Scheme 1). The mechanism in Scheme 1 thus indicates that  $[(\text{N-C}_6\text{H}_5\text{OETPP})\text{Fe}]^{2+}$  can be formed via both a slow and a rapid process.

**Migration Reactivities of Singly Oxidized Complexes.** The slow migration reaction of  $[(\text{OETPP})\text{Fe}(\text{C}_6\text{H}_5)]^+$  in Scheme 1 was confirmed by using an oxidant that can produce only the singly oxidized porphyrin. The one-electron reduction potential of ferricenium ion ( $\text{Fc}^+$ ;  $E_{\text{red}}^0 = 0.37 \text{ V}$ )<sup>35</sup> in MeCN is more positive than the first one-electron oxidation potential of  $(\text{OETPP})\text{Fe}(\text{C}_6\text{H}_5)$  ( $E_{\text{ox}(1)}^0 = 0.27 \text{ V}$ ) but less positive than the second one-electron oxidation potential ( $E_{\text{ox}(2)}^0 = 1.06 \text{ V}$ ).<sup>26</sup> Thus, only the singly oxidized complex,  $[(\text{OETPP})\text{Fe}(\text{C}_6\text{H}_5)]^+$ , can be produced by an electron transfer from  $\text{Fc}^+$  to  $(\text{OETPP})\text{Fe}(\text{C}_6\text{H}_5)$ . The addition of more than 2 equiv of  $\text{Fc}^+$  to an MeCN solution of  $(\text{OETPP})\text{Fe}(\text{C}_6\text{H}_5)$  slowly leads to  $[(N\text{-C}_6\text{H}_5\text{OETPP})\text{Fe}]^{2+}$  ( $\lambda_{\text{max}} = 486$  and  $721 \text{ nm}$ )<sup>26</sup> via an iron to nitrogen migration of the  $\text{C}_6\text{H}_5$  ligand following the initial rapid electron transfer from  $(\text{OETPP})\text{Fe}(\text{C}_6\text{H}_5)$  to  $\text{Fc}^+$ . The second electron transfer from the migrated product,  $[(N\text{-C}_6\text{H}_5\text{OETPP})\text{Fe}]^+$ , to  $\text{Fc}^+$  may occur rapidly to yield  $[(N\text{-C}_6\text{H}_5\text{OETPP})\text{Fe}]^{2+}$  as shown in Scheme 2, since the one-electron oxidation potential of  $[(N\text{-C}_6\text{H}_5\text{OETPP})\text{Fe}]^+$  ( $-0.25 \text{ V}$ )<sup>25,26</sup> is more negative than the one-electron reduction potential of  $\text{Fc}^+$  ( $0.37 \text{ V}$ ). The rate of formation of  $[(N\text{-C}_6\text{H}_5\text{OETPP})\text{Fe}]^{2+}$  obeys first-order kinetics (see Supporting Information). The first-order rate constant corresponds to the migration rate constant of the singly oxidized complex ( $k_{\text{mig1}}$ ), which would be independent of the oxidants provided that only the singly oxidized complex is produced by the electron transfer with the oxidants. This was confirmed by determining the rate constants for formation of  $[(N\text{-C}_6\text{H}_5\text{OETPP})\text{Fe}]^{2+}$  in the electron-transfer oxidation of  $(\text{OETPP})\text{Fe}(\text{C}_6\text{H}_5)$  with different concentrations of a series of ferricenium ion derivatives. Thus, the determined  $k_{\text{mig1}}$  values become independent of the concentration of the ferricenium ion derivative at concentrations larger than  $5 \times 10^{-4} \text{ M}$  as shown in Figure 2, where a plot of  $k_{\text{mig1}}$  vs the concentration of 1,1'-dimethylferricenium ion ( $\text{Me}_2\text{Fc}^+$ ) is given as an example. Furthermore, the  $k_{\text{mig1}}$  values are the same irrespective of the difference in oxidation potentials of the utilized ferricenium ion derivatives

(37) The electron transfer equilibrium is slightly endergonic judging from the difference in the one-electron redox potentials between  $[(N\text{-}C_6H_5\text{-}OETPP)Fe]^{3+}$  and  $[(OETPP)Fe(C_6H_5)]^+$ .

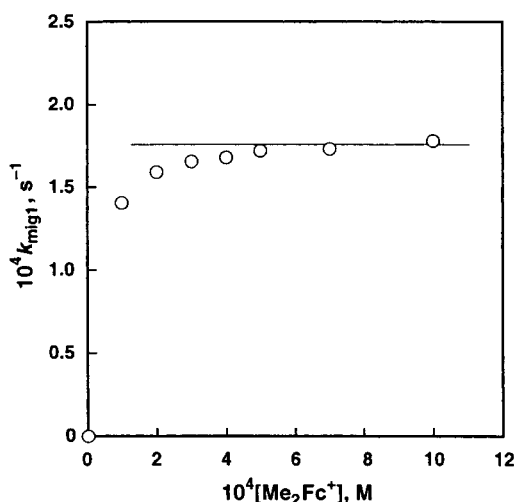


**Figure 2.** Plot of  $k_{\text{mig1}}$  vs  $[\text{Me}_2\text{Fc}^+]$  for the migration of the  $\text{C}_6\text{H}_5$  group from  $[(\text{OETPP})\text{Fe}(\text{C}_6\text{H}_5)]^+$  in deaerated MeCN at 298 K.

**Table 2.** Migration Rate Constants for  $\sigma$ -Bonded Groups (R) of  $[(\text{P})\text{M}(\text{R})]^+$  ( $k_{\text{mig1}}$ ) and  $[(\text{P})\text{M}(\text{R})]^{2+}$  ( $k_{\text{mig2}}$ )<sup>a</sup> and Utilized One-Electron Oxidants with Their Reduction Potentials

(P)M(R)	oxidant ( $E_{\text{red}}^0$ , V)	$k_{\text{mig1}}$ , <sup>b</sup> $\text{s}^{-1}$	$k_{\text{mig2}}$ , <sup>b</sup> $\text{s}^{-1}$
$(\text{OETPP})\text{Fe}(\text{C}_6\text{H}_5)$	$\text{Me}_2\text{Fc}^+$ (0.26)	$1.8 \times 10^{-4}$	
	$n\text{-BuFc}^+$ (0.31)	$1.8 \times 10^{-4}$	
	$\text{Fc}^+$ (0.37)	$1.8 \times 10^{-4}$	
	$\text{AcFc}^+$ (0.62)	$1.8 \times 10^{-4}$	
	$[\text{Ru}(\text{bpy})_3]^{3+}$ (1.24)		1.3
$(\text{OETPP})\text{Fe}(3,5\text{-C}_6\text{F}_2\text{H}_3)$	$\text{Fc}^+$ (0.37)	$4.2 \times 10^{-5}$	
	$[\text{Ru}(\text{bpy})_3]^{3+}$ (1.24)		0.39
$(\text{OETPP})\text{Fe}(\text{C}_6\text{F}_5)$	$\text{AcFc}^+$ (0.62)	$2.1 \times 10^{-5}$	
	$[\text{Ru}(\text{bpy})_3]^{3+}$ (1.24)		0.31
$(\text{TPP})\text{Co}(\text{CH}_3)$	$[\text{Fe}(\text{phen})_3]^{3+}$ (1.07)	$1.4 \times 10^{-2}$ <sup>c</sup>	
	$[\text{Ru}(\text{bpy})_3]^{3+}$ (1.24)		4.5
$(\text{TPP})\text{Co}(\text{C}_6\text{H}_5)$	$[\text{Fe}(\text{phen})_3]^{3+}$ (1.07)	$1.3 \times 10^{-3}$ <sup>c</sup>	
	$[\text{Ru}(\text{bpy})_3]^{3+}$ (1.24)		3.5
$(\text{TPP})\text{Co}(\text{C}_2\text{H}_5)$	$[\text{Fe}(\text{phen})_3]^{3+}$ (1.07)	$2.6 \times 10^2$ <sup>c</sup>	
$(\text{TPP})\text{Co}(n\text{-C}_4\text{H}_9)$	$[\text{Fe}(\text{phen})_3]^{3+}$ (1.07)	$1.2 \times 10^3$ <sup>c</sup>	

<sup>a</sup> Where P = OETPP or TPP and M = Fe or Co; in MeCN at 298 K. <sup>b</sup> The experimental error is within  $\pm 5\%$ . <sup>c</sup> Taken from ref 21.

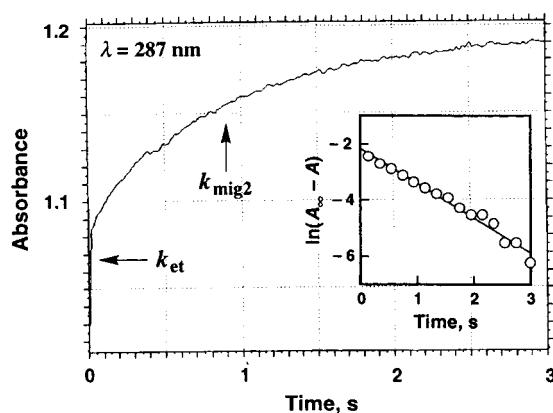


**Figure 3.** Time course of the absorption change at 287 nm due to formation of  $[\text{Ru}(\text{bpy})_3]^{2+}$  during the electron transfer from  $(\text{OETPP})\text{-Fe}(\text{C}_6\text{H}_5)$  ( $1.0 \times 10^{-5}$  M) to  $[\text{Ru}(\text{bpy})_3]^{3+}$  ( $3.0 \times 10^{-5}$  M) in deaerated MeCN at 298 K.

(see Table 2). Such a constant value confirms that the migration process is independent of the electron-transfer process (Scheme 2). The  $k_{\text{mig1}}$  value in Table 1 was confirmed to be essentially the same as the value obtained from the slow formation of  $[(N\text{-C}_6\text{H}_5\text{OETPP})\text{Fe}]^{2+}$  ( $\lambda_{\text{max}} = 721$  nm) in the second step in Figure 1.

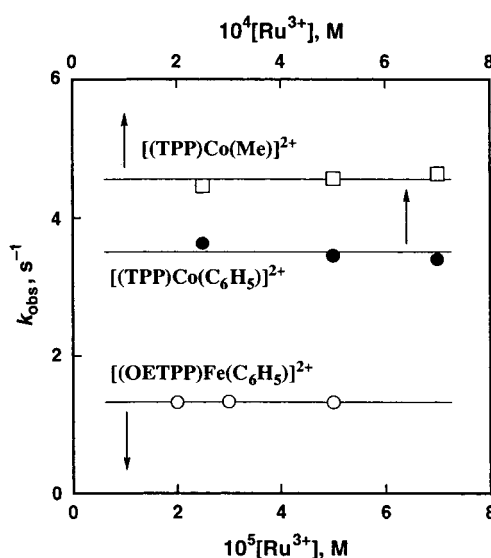
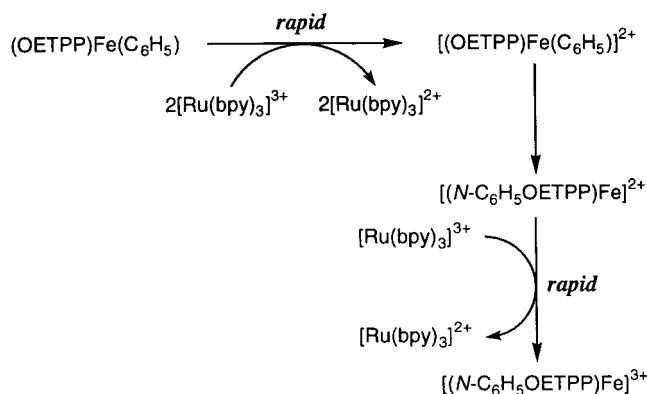
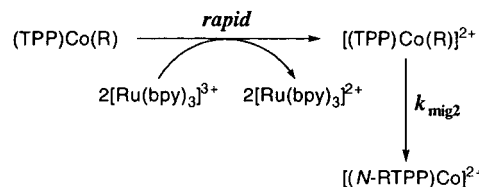


**Figure 4.** Plots of  $k_{\text{obs}}$  vs  $[\text{Ru}^{3+}]$  for the migration of the  $\sigma$ -bonded ligand from  $[(\text{TPP})\text{Co}(\text{Me})]^{2+}$  ( $\square$ ),  $[(\text{TPP})\text{Co}(\text{C}_6\text{H}_5)]^{2+}$  ( $\bullet$ ), and  $[(\text{OETPP})\text{Fe}(\text{C}_6\text{H}_5)]^{2+}$  ( $\circ$ ) in deaerated MeCN at 298 K.

### Scheme 3



### Scheme 4

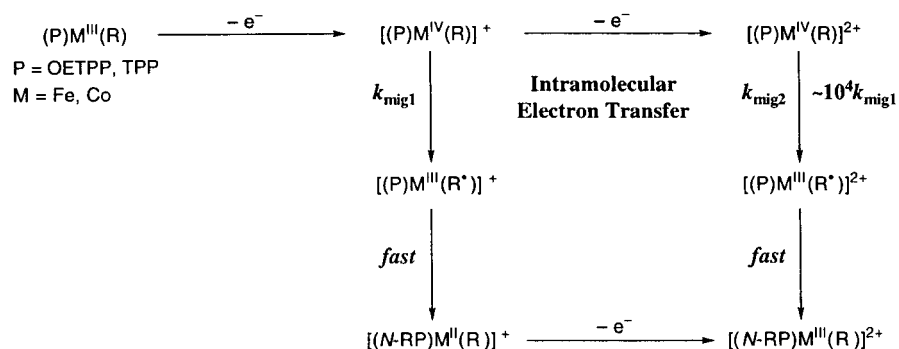


The  $k_{\text{mig1}}$  values of the singly oxidized fluorophenyl  $\sigma$ -bonded porphyrins  $[(\text{OETPP})\text{Fe}(\text{R})]^+$  ( $\text{R} = 3,5\text{-C}_6\text{F}_2\text{H}_2$  and  $\text{C}_6\text{F}_5$ ) were determined in a similar manner and the migration rate constants are also listed in Table 2. As expected, the  $k_{\text{mig1}}$  values decrease with increasing number of F substituents on the  $\sigma$ -bonded aryl group as the one-electron oxidation potential becomes more positive.

### Migration Reactivities of Doubly Oxidized Porphyrins.

The rapid migration of the phenyl group in the doubly oxidized  $[(\text{OETPP})\text{Fe}(\text{C}_6\text{H}_5)]^{2+}$  complex in Scheme 1 was monitored with the use of a stopped-flow technique. When more than 3 equiv of  $[\text{Ru}(\text{bpy})_3]^{3+}$  was employed for the oxidation of  $(\text{OETPP})\text{-Fe}(\text{C}_6\text{H}_5)$ , the rapid increase in absorbance at 287 nm due to  $[\text{Ru}(\text{bpy})_3]^{2+}$  formation<sup>27</sup> was accompanied by the two-electron oxidation of  $(\text{OETPP})\text{Fe}(\text{C}_6\text{H}_5)$ , followed by a slower increase in the  $[\text{Ru}(\text{bpy})_3]^{2+}$  absorbance as shown in Figure 3. Since the one-electron reduction potential of  $[\text{Ru}(\text{bpy})_3]^{3+}$  (1.24 V) is larger than the one-electron reduction potential of  $[(\text{OETPP})\text{-}$

Scheme 5



$\text{Fe}(\text{C}_6\text{H}_5)]^{2+}$  (1.06 V), the electron transfer from  $[(N\text{-C}_6\text{H}_5\text{-OETPP})\text{Fe}]^{2+}$  to  $[\text{Ru}(\text{bpy})_3]^{3+}$  in the presence of more than 3 equiv of  $[\text{Ru}(\text{bpy})_3]^{3+}$  should occur rather than the electron transfer to  $[(\text{OETPP})\text{Fe}(\text{C}_6\text{H}_5)]^{2+}$  in Scheme 1. Thus, migration of the phenyl group in the doubly oxidized complex,  $[(\text{OETPP})\text{Fe}(\text{C}_6\text{H}_5)]^{2+}$ , will become the rate-determining step following the initial two-electron oxidation of  $(\text{OETPP})\text{Fe}(\text{C}_6\text{H}_5)$  as shown in Scheme 3. In such a case, the migration rate can be determined from the rate of formation of  $[\text{Ru}(\text{bpy})_3]^{2+}$  in the second step of Figure 3. It was confirmed that there was no second-step formation of  $[\text{Ru}(\text{bpy})_3]^{2+}$  when 2 equiv of  $[\text{Ru}(\text{bpy})_3]^{3+}$  was employed in the reactions with  $(\text{OETPP})\text{Fe}(\text{C}_6\text{H}_5)$ . The second step leads to an increase in absorbance at 287 nm due to  $[\text{Ru}(\text{bpy})_3]^{2+}$ .<sup>38</sup> The rate obeys first-order kinetics and the observed first-order rate constants are independent of the  $[\text{Ru}(\text{bpy})_3]^{3+}$  concentration as shown in Figure 4. Thus, the first-order rate constant corresponds to the migration rate constant of the doubly oxidized complex,  $[(\text{OETPP})\text{Fe}(\text{C}_6\text{H}_5)]^{2+}$  ( $k_{mig2}$ ), as listed in Table 2. The  $k_{mig2}$  values of the doubly oxidized fluorophenyl  $\sigma$ -bonded porphyrins  $[(\text{OETPP})\text{Fe}(\text{R})]^{2+}$  ( $\text{R} = 3,5\text{-C}_6\text{F}_2\text{H}_2$  and  $\text{C}_6\text{F}_5$ ) were determined in a similar manner and these values are also listed in Table 2.

**Comparison of Migration Reactivities between Singly and Doubly Oxidized Porphyrins.** As shown in Table 2, the  $k_{mig2}$  value of doubly oxidized complex,  $[(\text{OETPP})\text{Fe}(\text{R})]^{2+}$ , decreases with increasing the number of F substituents on the  $\sigma$ -bonded phenyl group and at the same time the one-electron oxidation potential becomes more positive. A comparison of the migration rate constants for the singly oxidized complex ( $k_{mig1}$ ) with that of the doubly oxidized complex ( $k_{mig2}$ ) reveals a significant increase in the migration reactivity (ca.  $10^4$  times) upon formation of the doubly oxidized porphyrin as compared to the singly oxidized derivative.

We previously reported migration rate constants for the singly oxidized organocobalt porphyrins,  $[(\text{TPP})\text{Co}(\text{R})]^+$  ( $\text{R} = n\text{-C}_4\text{H}_9$ ,  $\text{C}_2\text{H}_5$ ,  $\text{CH}_3$ , and  $\text{C}_6\text{H}_5$ ), produced by the electron-transfer oxidation of  $(\text{TPP})\text{Co}(\text{R})$  with  $[\text{Fe}(\text{phen})_3]^{3+}$  (phen = 1,10-phenanthroline) in MeCN.<sup>21</sup> When  $[\text{Fe}(\text{phen})_3]^{3+}$  is replaced by a stronger oxidant,  $[\text{Ru}(\text{bpy})_3]^{3+}$ , the two-electron oxidation of  $(\text{TPP})\text{Co}(\text{R})$  becomes energetically feasible. Thus, migration rates of the doubly oxidized porphyrin  $[(\text{TPP})\text{Co}(\text{R})]^{2+}$ ,

produced by the two-electron oxidation of  $(\text{TPP})\text{Co}(\text{R})$  with  $[\text{Ru}(\text{bpy})_3]^{3+}$ , were determined by monitoring the change in UV-visible absorption as  $[(N\text{-RTPP})\text{Co}]^{2+}$  was generated.<sup>21</sup> The rate of  $[(N\text{-RTPP})\text{Co}]^{2+}$  formation during the two-electron oxidation of  $(\text{TPP})\text{Co}(\text{R})$  ( $\text{R} = \text{CH}_3$  and  $\text{C}_6\text{H}_5$ ) with a large excess  $[\text{Ru}(\text{bpy})_3]^{3+}$  obeys first-order kinetics in MeCN at 298 K. The observed first-order rate constant corresponds to the migration rate constant of  $[(\text{TPP})\text{Co}(\text{R})]^{2+}$  ( $k_{mig2}$ ) formed in the rapid two-electron oxidation of  $(\text{TPP})\text{Co}(\text{R})$  (Scheme 4). As shown in Figure 4, the  $k_{mig2}$  value is constant with change in the  $[\text{Ru}(\text{bpy})_3]^{3+}$  concentration for  $\text{R} = \text{CH}_3$  and  $\text{C}_6\text{H}_5$ , and these values are also listed in Table 2.

The  $k_{mig2}$  values of both investigated  $[(\text{TPP})\text{Co}(\text{R})]^{2+}$  complexes are about  $10^4$  times larger than the reported  $k_{mig1}$  values of the singly oxidized  $[(\text{TPP})\text{Co}(\text{R})]^+$  derivatives, which are also listed in Table 2.<sup>21</sup> In the case of  $\text{R} = \text{C}_2\text{H}_5$  and  $n\text{-C}_4\text{H}_9$ , the migration rates from the doubly oxidized complexes were so rapid as to fall outside the range of the stopped-flow method ( $>10^3 \text{ s}^{-1}$ ). This is also consistent with the large  $k_{mig1}$  values for  $\text{R} = \text{C}_2\text{H}_5$  and  $n\text{-C}_4\text{H}_9$ <sup>21</sup> in Table 2.

An interesting point to note from the results in Table 2 is that the magnitude of the enhanced rate in the migration reaction from the doubly oxidized cobalt and iron porphyrins as compared to the singly oxidized derivatives are about the same, ca.  $10^4$  times, irrespective of the  $\sigma$ -bonded ligand, the nature of the porphyrin, and the type of metal ion (iron or cobalt). Thus, it appears that the migration reactivities of  $\sigma$ -bonded organometallic porphyrins are significantly altered depending mainly on the oxidation state (singly or doubly oxidized). We have previously proposed that the migration occurs via an intramolecular electron transfer from the  $\sigma$ -bonded ligand to the metal ion resulting in a homolytic cleavage of the metal-carbon bond.<sup>21,24,39</sup> The enhanced migration reactivity of the doubly oxidized porphyrins, as compared to the reactivity of the singly oxidized complex, is also consistent with an intramolecular electron transfer for migration of the  $\sigma$ -bonded ligand as shown in Scheme 5. Although the metal(III)-carbon bond of  $(P)M^{III}(R)$  is stable, an intramolecular electron transfer from the  $\sigma$ -bonded ligand to the metal(IV) of the singly oxidized complex,  $[(P)M^{IV}(R)]^+$ , occurs leading to the migration, and such an intramolecular electron transfer is accelerated for the doubly oxidized complex,  $[(P)M^{IV}(R)]^{2+}$ , in which the porphyrin ligand (P) is oxidized,<sup>21,25-27</sup> and thereby the electron density on the metal may be further decreased due to the weaker coordination of the oxidized porphyrin ligand as compared to that of singly oxidized complex.

(38) The absorbance change at 287 nm (2 mm i.d.) due to the second-step formation of  $[\text{Ru}(\text{bpy})_3]^{2+}$  in Figure 3 corresponds to 1 equiv of  $(\text{OETPP})\text{Fe}(\text{C}_6\text{H}_5)$  ( $1.0 \times 10^{-5} \text{ M}$ ). According to Scheme 3, the initial absorbance change at 287 nm due to the rapid formation of  $[\text{Ru}(\text{bpy})_3]^{2+}$  by the two-electron oxidation of  $(\text{OETPP})\text{Fe}(\text{C}_6\text{H}_5)$  should be twice as much compared to that for the second step formation. However, only the partial change is observed for the first step ( $k_{et}$ ) in Figure 3 because of the rapid electron-transfer reaction occurring even during the mixing time.

(39) The homolytic cleavage of the M-C bond mainly results in the R group migration and a small fraction of the produced radical (5%) escapes to yield methane in the case of the oxidation of  $(\text{TPP})\text{Co}(\text{CH}_3)$ .<sup>21</sup>

**Acknowledgment.** This work was partially supported by an International Scientific Research Program grant (08044083) and Grants-in-Aid for Scientific Research Priority Area (10149230, 09237239, and 09231226) from the Ministry of Education, Science, Culture and Sports, Japan. R.G. acknowledges support from the CNRS. K.M.K. also acknowledges support from the Robert A. Welch Foundation (Grant E-680).

**Supporting Information Available:** Time course of the absorption change at 721 nm due to formation of  $[(N-C_6H_5OETPP)Fe]^{2+}$  after electron transfer from  $(OETPP)Fe(C_6H_5)$  to  $Fc^+$  together with the first-order plot (Figure S1) and tables for kinetic runs in Figures 2 and 4 (Tables S2 and S3, respectively). This material is available free of charge via the Internet at <http://pubs.acs.org>.

IC990324S